# Ultrasonic analysis and lock-in thermography for debonding evaluation of composite adhesive joints

NDT& E International pre-print https://dx.doi.org/10.1016/j.ndteint.2015.09.001

# ULTRASONIC ANALYSIS AND LOCK-IN THERMOGRAPHY FOR DEBONDING EVALUATION OF COMPOSITE ADHESIVE JOINTS

Palumbo D [1], Tamborrino R [2], Galietti U [1], Aversa P [2], Tatì A[3], Luprano VAM [2]

Corresponding author: Palumbo D., email: davide.palumbo@poliba.it

[1]*Department of Mechanics, Mathematics and Management (DMMM), Politecnico di Bari, Viale Japigia 182, 70126, Bari (Italy),*
[2]*Enea Centro Ricerche Brindisi, Strada Statale 7 Via Appia, 72100, Brindisi (Italy),*
[3]*Enea Centro Ricerche Casaccia, Via Anguillarese, 301, 00123, Roma (Italy)*

**Abstract**

Bonded joints provide a means of assembling that reduces the stress concentration. However, to ensure the joints have a good mechanical strength, is necessary to control various factors including the adhesion of the two surfaces of the joints.
Glass-fiber reinforced thermosetting plastic (GFRP) adhesive joints were characterized through ultrasonic imaging (UT C-Scan) and lock-in thermographic (LIT) analysis in order to assess the adhesion quality before being subjected to static tensile mechanical tests. Furthermore, samples of the same lot were subjected to accelerated aging cycles to evaluate their behaviour in temperate zones.
The mapping of each sample using non-destructive testing has been obtained. Visual testing were performed on all specimens after the mechanical tests in order to obtain a comparison with ultrasonic and lock-in thermography technique.
A quantitative analysis has been carried out to evaluate the ability of lock-in thermography in investigating inadequate bonding between the adherents and obtaining the validation of the technique by the consistency of the results with the well-established ultrasonic testing.

**Keywords:** Glass-fiber reinforced plastic (GFRP), adhesive joints, ultrasonic C-scan, lock-in thermography, hygrothermal aging

## 1. Introduction

Wind turbine blades are made from polymer composites to provide high specific stiffness, strength, and good fatigue performance. However, large composite structures are prone to manufacturing defects such as delamination and adhesive failure, which can lead to crack initiation and propagation [1].
Adhesive bonding failure is a key manufacturing defect typical of blade joined using adhesives paste of several millimeters thick. In fact, they can be expected to experience significant static and fatigue loads under various environmental conditions over their service life. National renewable energy laboratory, USA statistics shows in Fig.1 that manufacturing defects and in-service damages are the main reason for early blade failure [2].

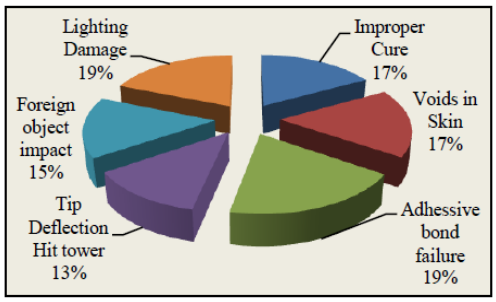


Figure 1: Blade damages at manufacturing and operational stage [2].

Despite great attention given to maintain quality in manufacturing processes, the data available for joints of this class with composite adherents indicate significant sensitivity to adhered properties and surface preparation, adhesive composition (chemistry, additives, mixing, curing), adhesive thickness, temperature, and moisture, as well as joint geometry [3].

Many researchers have done extensive work to identify different types of defects in adhesive joints and have suggested suitable non-destructive test methods to evaluate them [4–8].

Although, the influence of overlapped reflections, scattering and attenuation of the reflected ultrasonic waves from the multi-layered structure appears and the scattering effect also has a negative impact to the propagating ultrasonic waves and requires to use lower frequencies [9], ultrasonic methods have been widely used in the non-destructive testing and inspection of adhesive joints showing a high sensitivity to the defects commonly found in wind rotor blade.

The propagation characteristics of ultrasonic waves are used to determine material properties throughout the volume of turbine blade and to detect and characterize the surface and subsurface flaws and also are suitable for quality control and for estimation of the adhesion level between composite layers. The ultrasonic C-scan imaging can be used for the area mapping of the component [10]. C-scan is 2D image representation using ultrasonic wave signal acquired point-by-point as A-scan signal from the structure. For automated inspection, C-scan system consists of motorized scanner to move ultrasonic probe over the structure. Manual A-scan provides qualitative information whereas C-scan provides quantitative information about damage extent, type of damage etc [11].

Thermal techniques can be also used to investigate defects in adhesively bonded components [12], [13]. Stimulated Thermography is able to detect defects in homogeneous materials thanks to different thermal behavior that they have if subjected to a thermal stimulation. This behavior is due to the different thermal- physical properties involved in the heat transmission phenomena such as the thermal conductivity, the heat capacity at constant pressure and the density of material [12], [13].

In literature many works regard the application of stimulated thermography for the NDE of FRP strengthening system bonded on concrete structures [14-16]. In these works it was shown the capability of thermography for the estimation of defects and the strong and weak points with respect to other NDT techniques were highlighted.

The ability of thermography to characterized defects in adhesively bonded composite joints was demonstrated in various works [17], [18]. In particular, Genest *et al.*, [19] used flash thermography and a novel signal processing to improve the debond visibility and reduces the influence of the repair edges. The new technique was demonstrated considering simulated and

real (debonding) in CFRP bonded patches. Quantitative analysis shows results in good agreement with ultrasonic and destructive technique.
In the work of Schroeder *et al.*, [20] Pulsed Thermography was used to evaluate large automotive assemblies, composite parts and bonded joints. All tests were carried out with Flash Thermography technique that requires short cycle time and then can be used for on-line tests for part validation.
Johnson [21] proposes a new approach based on TSA (Thermoelastic Stress Analysis) technique to characterized the damage initiation and progression in FRP single lap shear joints. This technique allows to obtain information about the damage extent of material and can be used for the monitoring of damage during the fatigue test.
In this paper we analyze, the results of an experimental investigation aimed at determining the capability and reliability of the lock-in thermography [12], [13], [22], [23] as a non-destructive method of assessing the integrity of glass-fiber reinforced thermosetting plastic (GFRP) adhesive joints used for the construction of wind rotor blades.
Different tests were carried out on single lap adhesive joints designed according to ASTM D 3165 [24], using lock-in thermography and ultrasonic C-scan technique. It was carried out a quantitative analysis in order to evaluate the ability and the advantages of lock-in thermography with respect to the ultrasonic C-scan technique that is considered well established in literature for the debonding detection of joints.

## 2.Materials and methods

### *2.1 Specimens*

Single lap adhesive joints were prepared as per ASTM D 3165 [24] standard using glass fiber reinforced thermosetting plastic (vinyl ester GFRP) as substrate and a two part epoxy adhesive: AME6000 INF (Ashland Composite Polymers) and ADH 90.91 (Altana Electrical Insulation). Adherends were characterized by multiple layers of quadriaxial 0 ° / +45 ° / 90 ° / -45 ° fabric glass fiber and were obtained from a laminate fabricated using the technique of infusion of the resin under vacuum (VARI). Surface preparation was carried out according to ASTM D 2093 [25] standard for surface preparation of plastics. The panels, properly cleaned and treated, were placed inside a tool for bonding where they were lined up by reference pins. After spreading a thin layer of adhesive, the assembly was closed and the pressure was applied. As regards the conditions of care, they are observed as indicated by the manufacturer of adhesive.
The planar and three-dimensional geometry of the joints are shown in Figure 2.
The single-lap samples were cut from the panels according to scheme imposed by ASTM D 3165.
Since the legislation provided for the use of metals, while the present study is based on adherends in composite materials, changes have been made, in the thickness of the adherends, which are set to a value of 2.5 mm, while the thickness of the adhesive remains equal to 0.76 mm.
A total of 12 single lap joints were used for the experimental tests and they were denoted by the initials VA followed by a sequential cardinal number and the indication of the production lot.

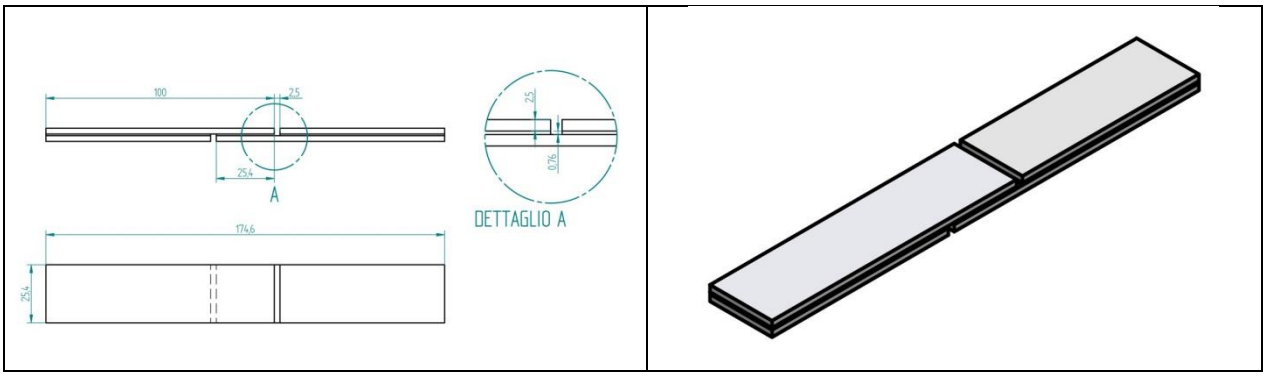

Figure 2: Planar and three-dimensional geometry of the joints

### *2.2 Hygrothermal aging*

The aging cycles for testing were determined on the basis of the monthly average of maximum temperature, minimum temperature, and moisture percentage of the last thirty years in Alpine and Apennines Italian region at about 1500 meters above sea level. The cycle time was 4 months. Within 24 hours there were 3 sub-cycles, which had been assigned a specific weight according to their average duration in a year. The sub-cycles were:

- Cool: the temperature was set to the average of the minimum of the months January, February, March, October, November, December, which was -6 ° C;
- Mild: the temperature was set to the average of the maximum of the months of April and September, corresponding to 5 ° C;
- Warm: the temperature was set to the average of the maximum of the months of May, June, July, August, or 15 ° C.

Figure 3 shows the daily cycle of aging.

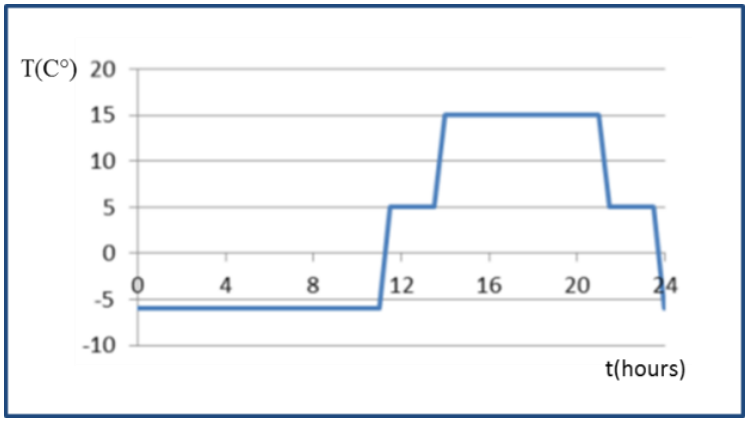

Figure 3. Daily hygrothermal aging: cool, mild and warm sub-cycles within 24 hours

The described accelerated aging was implemented in a climatic chamber.
The 12 adhesive joints studied in this paper were aged for 4 months.

### *2.3 Ultrasonic testing*

Before carrying out thermographic and mechanical testing, all single-lap joint sample were subjected to a volumetric UT scanning analysis procedure. The ultrasonic inspections were performed with an automatic acquisition system developed in the laboratories of ENEA and available in the Brindisi Research Center. The system, by means of a management software implemented in LabVIEW$^{TM}$, acquires the radio-frequency signal (RF) coming from the instrument through the UT oscilloscope and controls a movement system (two axes at a time) in order to associate the RF signal with the spatial position. At the end of scan, UT data are saved in files containing the whole set of complete UT waveforms. From the UT file, UT images for any portion of the material thickness can be obtained and analyzed. The software allows the visualization in the A-Scan, B-Scan, C-Scan mode.
The experimental apparatus consists of the following elements:

- digital oscilloscope generating the voltage pulses, acquisition, visualization and digitalization of UT pulses;
- transmitter/receiver UT probe;
- PC for UT data processing and mechanical displacement control;
- mechanical displacement system, consisting of a 3-axis for UT probe motioning and control;
- immersion pump for coupling ultrasound with driven jets of water.

The UT inspection technique chosen for this study was the "pulse - echo" and the coupling of ultrasound has been realized with driven jets of water. This choice was necessary to avoid the specimen to stay in the water for not altering the physical and chemical characteristics and for preventing the absorption of water in the material. The probe for this application was a focused immersion transducer of 1 MHz frequency. Water and GFRP material UT speed were 1483m/s and 2578m/s, respectively. The correct focal distance, to focus the UT beam at mid joint, has been established experimentally evaluating the maximum amplitude of the reflected signal.
For each single lap joint sample, a 80 mm x 24 mm area over the bonding was scanned with a 0.2 mm scan step (Figure 4).
The UT scanning was performed before aging the joints and after 4 months aging.

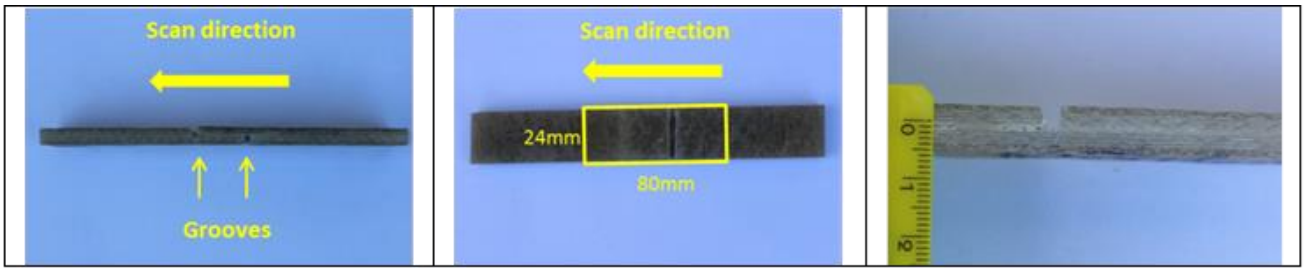


Figure 4. Scan direction and scanned area

### *2.4 Lock-in thermographic analysis*

Lock-in thermography is based on the generation of thermal waves inside the specimen, for example, by depositing heat periodically on the specimen surface [12], [13]. The resulting oscillating temperature field in the stationary regime can be recorded remotely through its thermal infrared emission by an IR camera. Thermal wave can be reconstructed by measuring temperature evolution over the specimen surface: by a suited algorithm, information about magnitude ($A$) and phase ($\varphi$) of the thermal wave can be obtained.
Phase data are relatively independent of local optical and infrared surface features and phase signal allows to penetrate deeper into the material than the analysis of the magnitude signal.
In the phase image, the defects appear with a different phase signal respect to the homogeneous material. Moreover, the phase of thermal wave is related directly to depth $z$ [13]:

$$\varphi(z) = \frac{2\pi z}{\lambda} = \frac{z}{\mu} \tag{1}$$

with $\lambda$ thermal wavelength and μ the thermal diffusion length:

$$\mu = \sqrt{\frac{2k}{\omega \rho c_p}} = \sqrt{\frac{2\alpha}{\omega}} \tag{2}$$

where $k$ is the thermal conductivity, $\rho$ is the density, $c_p$ is the specific heat at constant pressure, $\omega$ is the modulation frequency and $\alpha$ is the thermal diffusivity.
Eq. (1) indicates that higher modulation frequencies restrict the analysis in a near-surface region, while low-frequency thermal waves propagate deeper but very slowly [13].
Lock-in thermography tests were performed by IR camera Flir 640 with thermal sensitivity (NETD) < 30 mK and based on a microbolometer detector with 640×512 pixels.
The set-up used is shown in Figure 5 (β = 30°, DT = 30 cm, DL = 20 cm). In particular two halogen lamps with power 500 W were controlled by MultiDES® system in order to heating specimens with a series of sinusoidal waves. Thermal data were processed by IRTA® software in order to obtain amplitude and phase images.

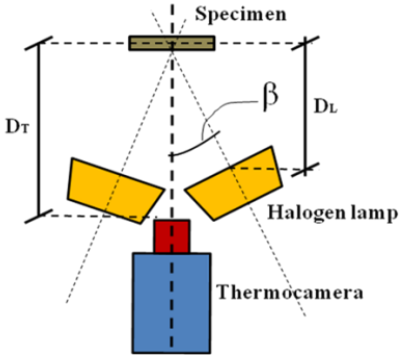


Figure 5. Top view of set-up used for lock-in thermography (β = 30°, DT = 30 cm, DL = 20 cm)

### *2.5 Mechanical tests*

Mechanical tests were conducted according to ASTM D3039 [26]. The tests were carried out at room temperature on the electromechanical machine MTS model Alliance RT/50 available in

the laboratory of mechanical tests ENEA. In mechanical testing, bonded joints are loaded to the point of breaking. The rupture of the specimens allowed to validate the results of non-destructive investigations. The broken joints have been visually inspected to locate correctly the defects highlighted with non-destructive controls. Anyway, mechanical tests, so accurately conducted, and their quantitative results will be the subject of a future work.

## 3. Results and discussion

### *3.1 Ultrasonic C-scan results*

The 1 MHz probe have allowed the complete UT signal penetration of the single-lap joints and the bonded area is reliably observed in the UT images .
All UT images are obtained selecting the distance of the slice from the probe, calculated by the software using the wave propagation speed and the time of flight, corresponding to the joint adhesive layer immediately over the first interface.
C-scan images of the section of interest show, according to the scale, areas with a great amplitude of the reflected signal, and areas with low amplitude of the signal.
The first are indicative of areas in which the bonding has occurred, then the adhesive layer is present. The signal, despite having undergone reflections to the first interface adhering/ adhesive and despite having attenuated crossing the composite material, propagates to adhesive thickness reaching the second adhering/adhesive interface where it was reflected. The signals having low amplitudes indicate areas associated with defects in the adhesive layer. Indeed, in this case the signal has been completely reflected at the first interface adhering/adhesive.
The images make us appreciate significant bond defects in all investigated sample.
In Figure 6, UT images from C-scan of no aged (UT0) and aged (UT4) single-lap joint samples are reported.
C-scan images of the section of interest show, according to the scale, areas with a great amplitude of the reflected signal, and areas with low amplitude of the signal. Comparing the images, before and after the aging of the same sample, does not appear any variation in the bonding. The comparison suggests that the adhesives yield the same bond quality.

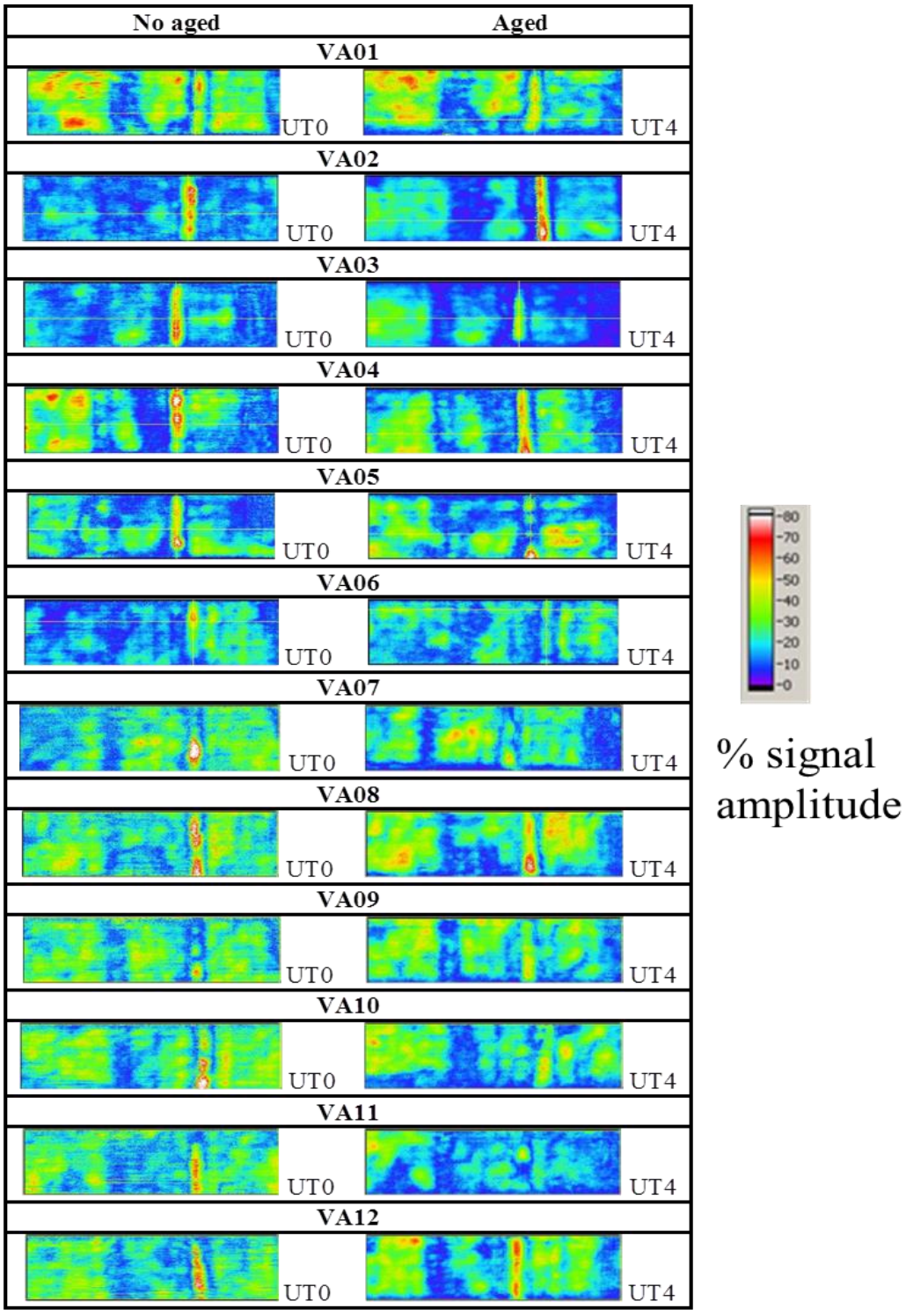


Figure 6. UT images from C-scan of no aged (UT0) and aged (UT4) single-lap joint samples

### *3.2 Lock-in thermography results*

Lock-in tests were carried out considering only one side of specimen and then defect was detected at the first interface adhering/adhesive. Different preliminary tests were carried out on a reference sample specimen, called VA0, in order to assess the optimum value of the modulation frequency for lock-in thermography tests. Debonded area it was simulated by

means of a teflon foil inserted between the adhesive and the adherent. As example, in Figure 7 is shown the phase image obtained with a modulation frequency of 0,0125 Hz on the sample specimen VA0.
The optimum modulation frequency was chosen as the one that gave higher phase contrast $|\Delta\varphi|$ determined as follows:

$$|\Delta\varphi| = |\varphi_{mA_1} - \varphi_{mA_2}| \tag{3}$$

$$\varphi_{mA_1} = mean[A_1] \qquad \varphi_{mA_2} = mean[A_2] \tag{4}$$

where $A_1$ and $A_2$ are respectively defected and sound areas and $\varphi_{mA1}$ and $\varphi_{mA2}$ are the mean values of the phase on areas $A_1$ and $A_2$, Figure 7.

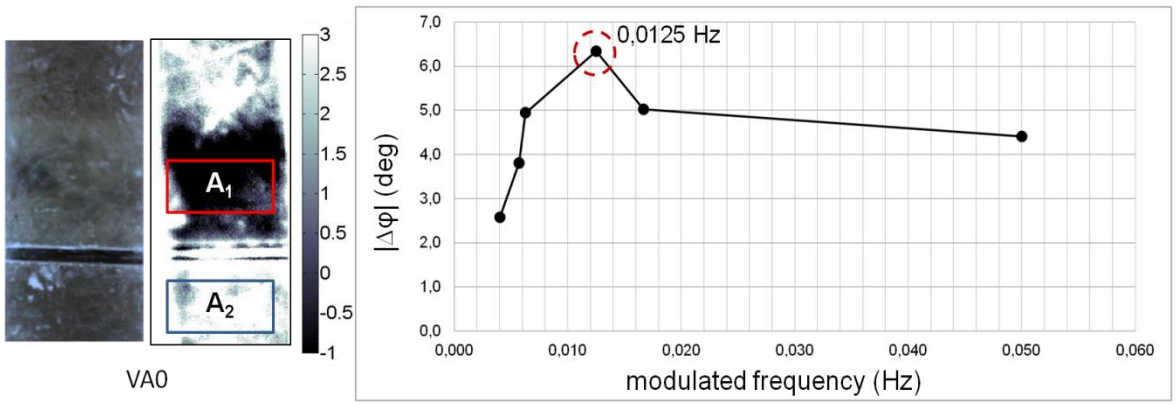


Figure 7: Evaluation of the maximum phase contrast by tests carried out on sample specimen VA0. $A_1$ and $A_2$ are respectively defected and sound areas considered for the evaluation of phase contrast.

As shown in Figure 7, 6 different modulation frequencies were used and the max value of phase contrast was obtained in correspondence of 0,0125 Hz. This frequency was then used for all lock-in thermography tests.
Figure 8 shows the phase images obtained by IRTA® software of all specimens before the aging. Black areas indicate the presence of bond defects while green lines delimitate the area of interest. Almost all specimens seem affected by debonding.

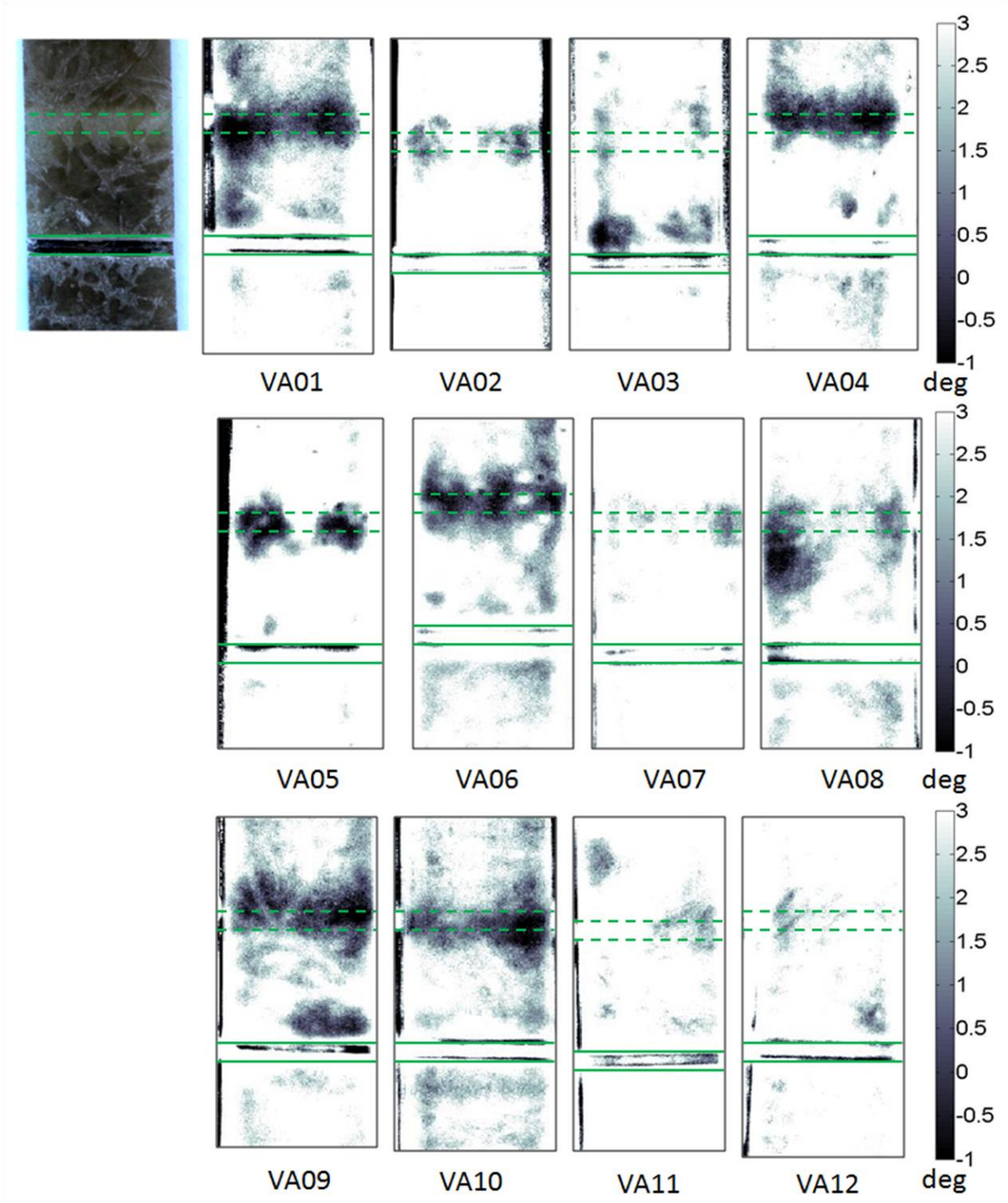


Figure 8: Phase images obtained with the modulation frequency 0,0125 Hz.

## 4. Discussion of results

### *4.1 Quantitative data analysis*

The quantitative thermographic and UT data analysis was carried out in order to identify the defects using a decision threshold values criterion [27]. In this way, the detectable and

undetectable defects are expressed as 1 and 0 (hit/miss data), respectively and it is possible a comparison between techniques.
In this work, the threshold value *Th* was defined through a statistical analysis of data considering the following equation [27]:

$$Th = \mu \pm n\sigma \qquad n = 1,2,.....N \tag{5}$$

where $\mu$ is the average value of signal measured in the healthy area of material, $\sigma$ is the standard deviation of the signal measured in the sound area of material and $n$ is a integer number that indicates the width of the confidence intervals.
From the previous paragraphs, both techniques detect, in section of interest between the two grooves, on the specimen VA11, entirely non defected area, thus it was considered as reference for *Th* evaluation. Figure 9 shows the total area *At* used to evaluate mean value and standard deviation of phase and UT data (square dotted line). In particular, indicating with 1 the detected defect and 0 the undetectable one, the hit/miss response is obtained by the following relations:

$$\begin{cases} \varphi \le Th = \mu - n\sigma \Rightarrow 1 \\ \varphi > Th = \mu - n\sigma \Rightarrow 0 \end{cases} \text{ for phase data, } \quad \begin{cases} s \le Th = \mu - n\sigma \Rightarrow 1 \\ s > Th = \mu - n\sigma \Rightarrow 0 \end{cases} \text{ for UT data} \tag{6}$$

where $\varphi$ is the phase signal (degree) and $s$ is the UT signal expressed as % signal amplitude.
The area *At* was also considered to quantify the equivalent damage due to debonding defects. In fact, if different debonded areas are present within the total area *At*, an equivalent debonded area can be assessed by hit/miss phase data as follows:

$$A_d = \sum_{i}^{N} \sum_{j}^{M} \varphi(i, j) \tag{7}$$

where *N* and *M* represent the number of rows and columns of the pixel matrix related to the area *At*. In these terms, an expression of equivalent debonded area normalized with respect to *At* area can be provided:

$$A_d\,\% = \frac{\sum_{i}^{N} \sum_{j}^{M} \varphi(i, j)}{A_t} * 100 \tag{8}$$

while the equivalent normalized bonded area can be defined as:

$$A_b\,\% = \frac{\left[ A_t - \sum_{i}^{N} \sum_{j}^{M} \varphi(i, j) \right]}{A_t} * 100 \tag{9}$$

Equations (7), (8), (9) can be written in similar way for UT data substituting $\varphi$ with $s$. *At* is composed by 8064 pixels for phase data and by 12000 pixels for UT data, Figure 9.
For both techniques $n$ value was assessed as the smallest number that gives a null defect for the specimen VA11. The $n$ values that provide an $A_b$% area close to 100% for phase and UT data are respectively 3 and 2.

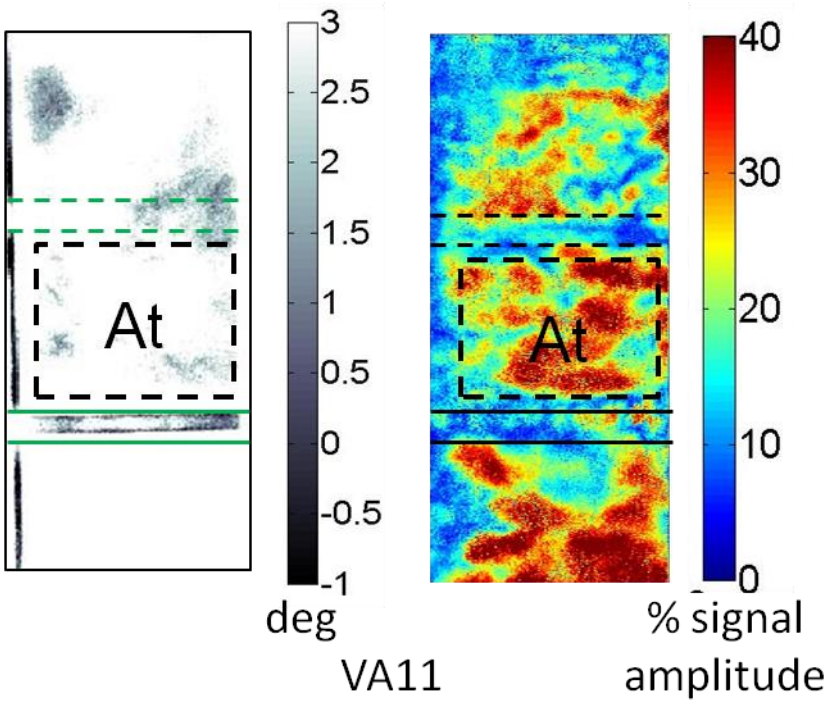


Figure 9: Area (*At*) considered to evaluate the equivalent debonded defect area on phase (left) and UT (right) data.

### *4.2 Comparison between Lock-in thermography and UT technique*

The comparison of images of both NDT techniques, grouped in figure 7 and figure 10, shows a good visualization of defects, allowing us to know their shape and dimensions. Lock-in Thermographic results agree with the ultrasonic inspection, thus its capability to locate and identify defects into bonded joints caused by environmental exposures or manufacturing process can be qualitatively assessed.
As always in NDT, the thermographic (lock-in) technique must be quantitatively validated by a rigorous mathematical argument. Phase images and ultrasonic images processed using the chosen threshold value criterion show almost the same equivalent normalized bonded area (Figure 10). The small difference in percentage can be attributed to measurement errors and to the use, however, of different techniques.
A further validation of the results of both non-destructive investigation comes from visual inspection of the broken specimens. For samples whose images give a response symptomatic of the absence of imperfections in bonding (white areas), the observation of the optical photos after the breakup confirms the goodness of the bonding, as in the case of samples that show the presence of defects (black areas and dotted lines on optical photos), which appear located in the

identified positions and with correct shapes and size. In Figure 11, pictures of the broken specimens are reported in comparison with the non-destructive results.

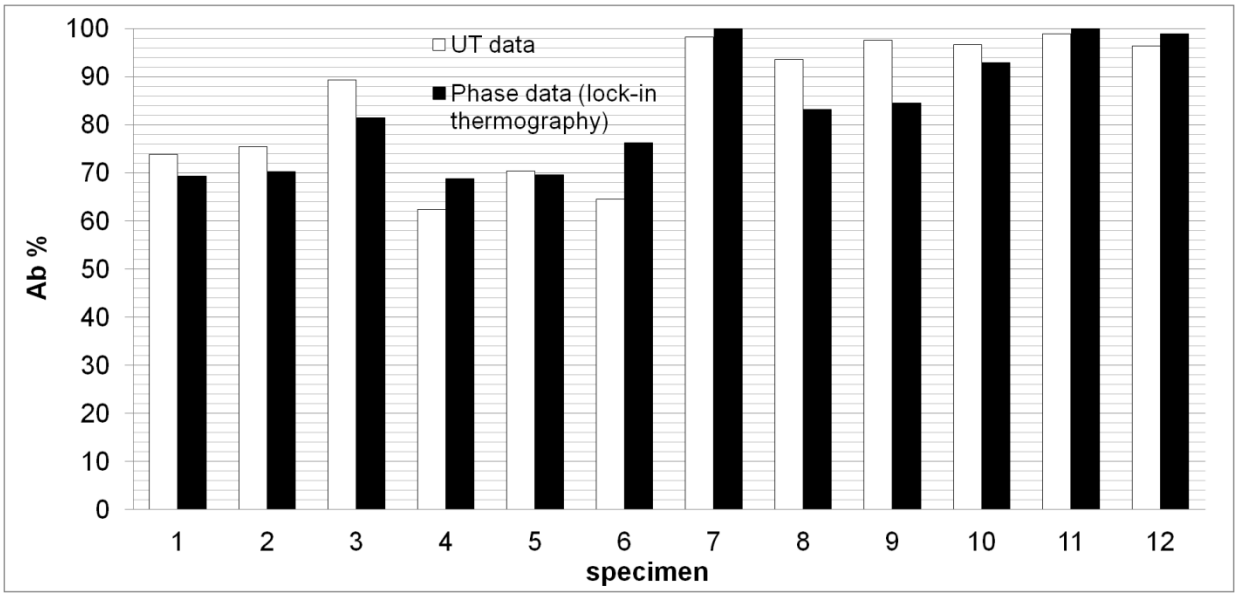


Figure 10. Comparison of equivalent normalized bonded area calculated for both techniques

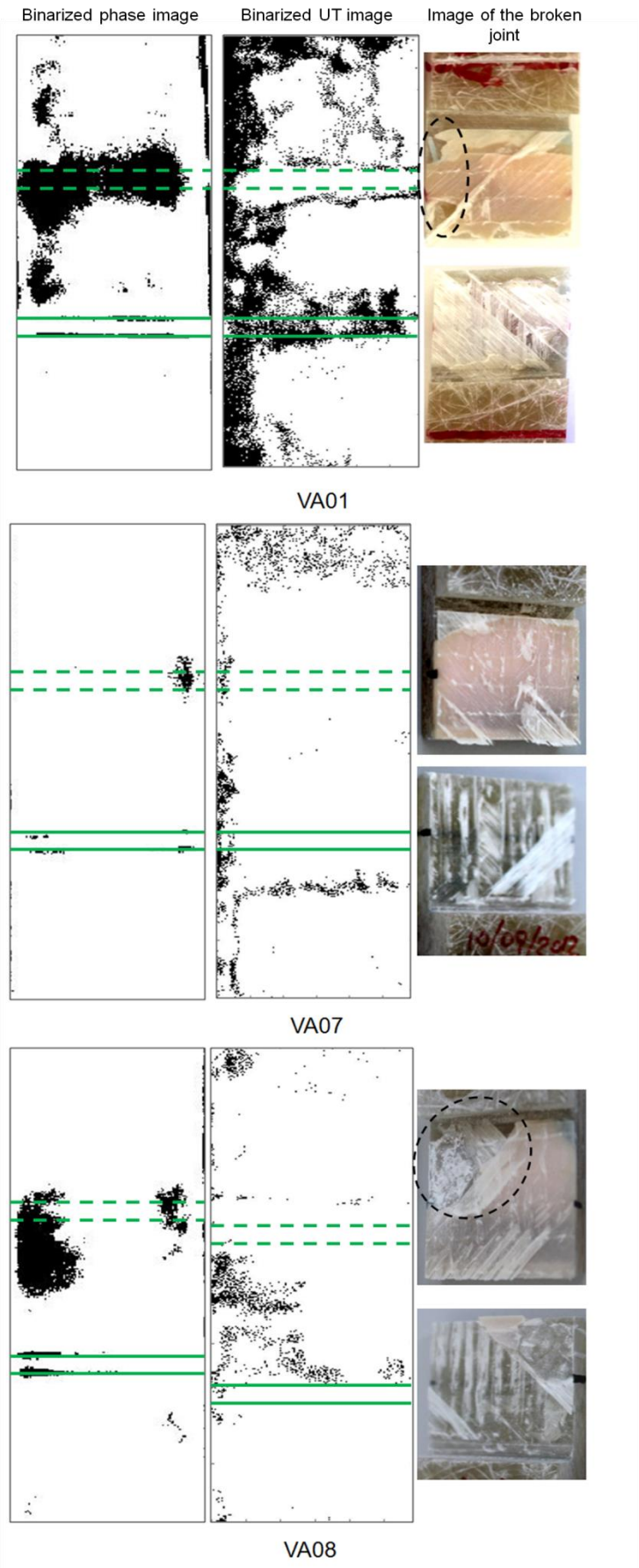


Fig 11: Binarized phase images, binarized UT images and images of the broken joints of the samples VA01, VA07, VA08

## 5. Conclusions

In the present work the results of an experimental activity have been presented and discussed to determine the capability and reliability of lock-in thermographic techniques as non-destructive testing for the debonding evaluation in glass-fiber reinforced plastic joints.
Different tests were carried out either with lock-in thermography and UT, on single lap adhesive joints designed according to ASTM D3165, before and after a cycle of accelerated aging. Both techniques confirm the presence of defects which were found without an appreciable change in their size and shape.
Ultrasonic C-scan tests were also used in order to validate thermographic results. In this regard, a quantitative analysis was carried out using a decision threshold values criterion. Lock-in thermography provides results in good agreement with UT C-scan inspection and besides, visual inspection, after the rupture of the sample, provides evidence of the results of non-destructive investigations.
Lock-in thermography has shown itself to be an excellent NDT tool to evaluate the condition of an initial, as-manufactured, bonded composite assembly, as well as an effective tool to follow part performance under various environmental conditions. Lock-in thermography can provide information with respect to the 'correctness' of the manufacturing process and can give indication of where the process might be improved.

## References


[1] Galappaththi UIK, De Silva AM, Draskovic M, Macdonald M, Strategic Quality Control Measures to Reduce Defects in Composite Wind Turbine Blades. International Conference on Renewable Energies and Power Quality (ICREPQ'13), Bilbao (Spain), 2013.

[2]NENUPHAR, Wind farms designed for the offshore environment, June 2010, ABM Centre, 128 rue du Faubourg de Douai, 59000 LILLE – FRANCE.

[3]Mandell JF, Cairns DS, Samborsky DD, Morehead RB, Haugen DJ, Prediction of Delamination in Wind Turbine Blades Structural Details. J. Sol. Energy, 2003; 125(4):522-9.

[4]Adams RD, Drinkwater BW, Non destructive testing of adhesively bonded joints. NDT & E International, 1997; 30(2):93-6.

[5]Dukes WA, Kinloch AJ, Non destructive testing of bonded joints, an adhesion science viewpoint, Non-Destructive Testing, 1974; 7:324-3.

[6]Segal E, Rose JL, Non-destructive testing of adhesive bond joints. Research Techniques in Nondestructive Testing, 1980; Vol. 4, Chapter 8, Academics press, London.

[7]Adams RD, Cawley P, Defects types and non-destructive testing techniques for composites and bonded joints, Construction and Building Materials, 1989; 3:170-14.

[8]Marquez FPG, Tobias AM, Perez JMP, Papaelias M, Condition monitoring of wind turbines: Techniques and methods. Renewable Energy, 2012; 46:169-10.

[9]Gieske JH, Rumsey MA, Nondestructive evaluation (NDE) of composite/metal bond interface of a wind turbine blade using acousto-ultrasonic technique. ASME wind energy symposium, W.Musial and D.E. Berg, eds., AIAA/ASME, 1997; 249-6.

[10] Raisutis R, Jasiuniene E, Sliteris R, Vladisauskas A, The review of non destructive techniques suitable for inspection of the wind turbine blades. Ultragarsas (Ultrasound), 2008; 63.

[11] Avinash SH, Singh NG, Makarand J, Damage detection methodology using ultrasonic non-destructive testing for composites structures. Proceedings of the National Seminar & Exhibitionon Non-Destructive Evaluation, NDE 2011, 2011.

[12] Maldague X, Applications of infrared thermography in non-destructive evaluation. Universitè Laval, Quebec City (Quebec), G1K 7P4, Canada, 2000.

[13] Maldague X, Theory and practice of infrared technology for non-destructive testing. Wiley Series in microwave and optical engineering, Kai Chang, Series Editor, 2001.

[14] Galietti U, Luprano V, Nenna S, Spagnolo L, Tundo A, Non-destructive defect characterization of concrete structures reinforced by means of FRP. Infrared Physics & Technology, 2007; 49:218-6.

[15] Tashan R, Al-mahaidi R, Investigation of the parameters that influence the accuracy of bond defect detection in CFRP bonded specimens using IR thermography. Composite Structures, 2012; 94:519-133.

[16] Taillade F, Quiertant M, Benzarti K, Aubagnac C, Shearography and pulsed stimulated infrared thermography applied to a nondestructive evaluation of FRP strengthening systems bonded on concrete structures. Construction and Building Materials, 2011; 25:568-7.

[17] Omar M, Hassan M, Donohue K, Saito K, Alloo R, Infrared thermography for inspecting the adhesion integrity of plastic welded joints. NDT & E International, 2006; 39:1-7.

[18] Berglind H, Dillenz A, Detecting glue deficiency in laminated wood – a thermography method comparison. NDT & E International, 2003; 36:395-5.

[19] Genest M, Martinez M, Mrad N, Renaud G, Fahr A, Pulsed thermography for non-destructive evaluation and damage growth monitoring of bonded repairs. Composite Structures, 2009; 88:112-9.

[20] Schroeder JA, Ahmed T, Chaudhry B, Shepard S, Non-destructive testing of structural composites and adhesively bonded composite joints: pulsed thermography. Composites: Part A, 2002; 33:1511-8.

[21] Johnson S, Thermoelastic stress analysis for detecting and characterizing static damage initiation in composite lap shear joints. Composites: Part B, 2014; 56:740-9.

[22] Meola C, Carlomagno MG, Squillace A, Vitiello A, Non-destructive evaluation of aerospace materials with lock-in thermography. Engineering Failure Analysis, 2005; 13:380-9.

[23] Montanini R, Freni F, Non-destructive evaluation of thick glass fiber-reinforced composites by means of optically excited lock-in thermography. Composites: Part A, 2012; 43:2075-8.

[24] ASTM D3165: Standard Test Method for Strength Properties of Adhesives in Shear by Tension Loading of Single-Lap-Joint Laminated Assemblies, 2004.

[25] ASTM D2093: Standard Practice for Preparation of Surfaces of Plastics Prior to Adhesive Bonding, 2004.
[26] ASTM D3039: Standard Test Method for Tensile Properties of Polymer Matrix Composite Materials, 2004.
[27] Palumbo D, Ancona D, Galietti U, Quantitative damage evaluation of composite materials with microwave thermographic technique: feasibility and new data analysis. Meccanica, 2015; 50:443-17.